

Supporting Information

Sample Name		TiN-0.5	TiN-1	TiN-1.25	TiN-1.5	TiN-1.75
Reactant	Tm/Yb@Nd/Yb@TiO ₂ weight (mg)	20	20	20	20	20
	Urea weight (mg)	10	20	25	30	35
Weight ratio of urea to Tm/Yb@Nd/Yb@TiO ₂		0.5	1	1.25	1.5	1.75
Actual N element in the TiO ₂ shell (at %)		0.44	0.83	1.07	1.38	1.56

Table S1 The content of N doping in the Tm/Yb@Nd/Yb@N-TiO₂ NPs prepared with different weight ratios of urea to Tm/Yb@Nd/Yb@a-TiO₂ precursor (a- means amorphous). The actual N doping amount was determined by XPS analysis. Note that most urea was thermally decomposed and only a few elemental N were doped in the TiO₂ shell.

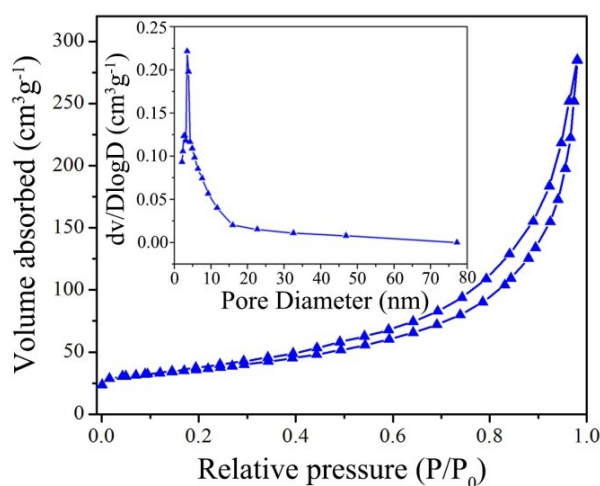


Figure S1. BET data and pore size distribution of the Tm/Yb@Yb/Nd@N-TiO₂ NPs. This result confirms that the N-TiO₂ shell has many nanoporous pores and a large surface area.

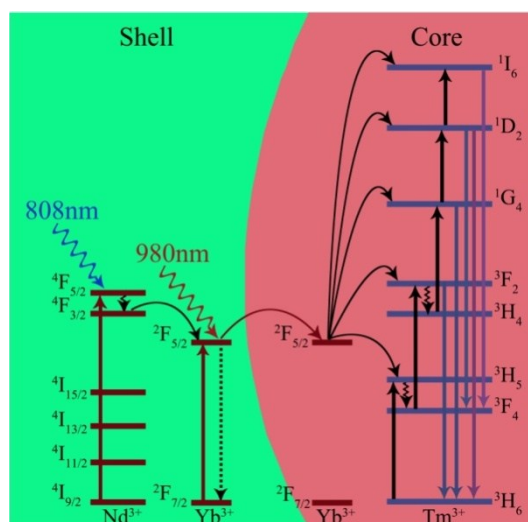


Figure S2. Energy levels of Tm^{3+} - Yb^{3+} - Nd^{3+} ions in the core-shell UCNs and energy transfer pathways for their UC emissions upon NIR excitation.

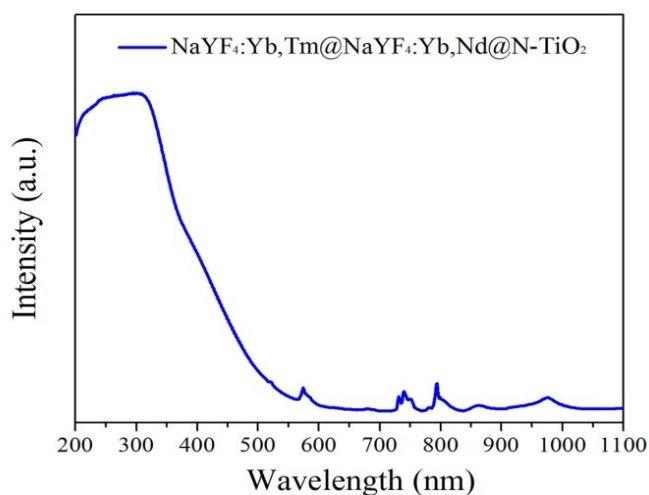


Figure S3. UV-Vis-NIR absorption spectrum of the $\text{Tm}/\text{Yb}@/\text{Yb}/\text{Nd}@/\text{N-TiO}_2$ NPs. The nanocomposite has a strong absorption in the UV and short Vis region (< 550 nm) due to the N-doped TiO_2 shell, which overlaps all the upconverted UV and Vis emissions from the $\text{Tm}/\text{Yb}@/\text{Yb}/\text{Nd}$ NCs (see Fig. 5).

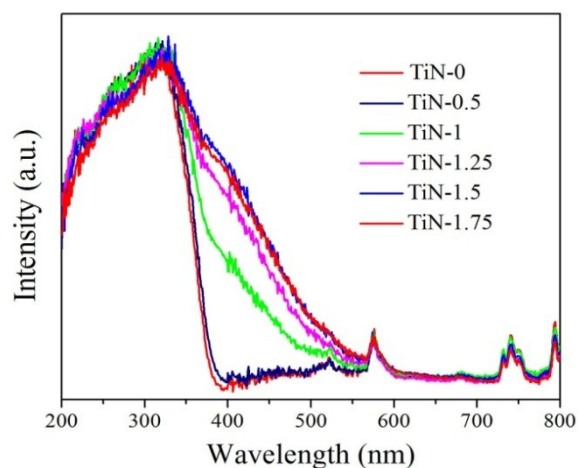


Figure S4. UV-Vis spectra of the Tm/Yb@Yb/Nd@N-TiO₂ NPs doped with different amount of N element.

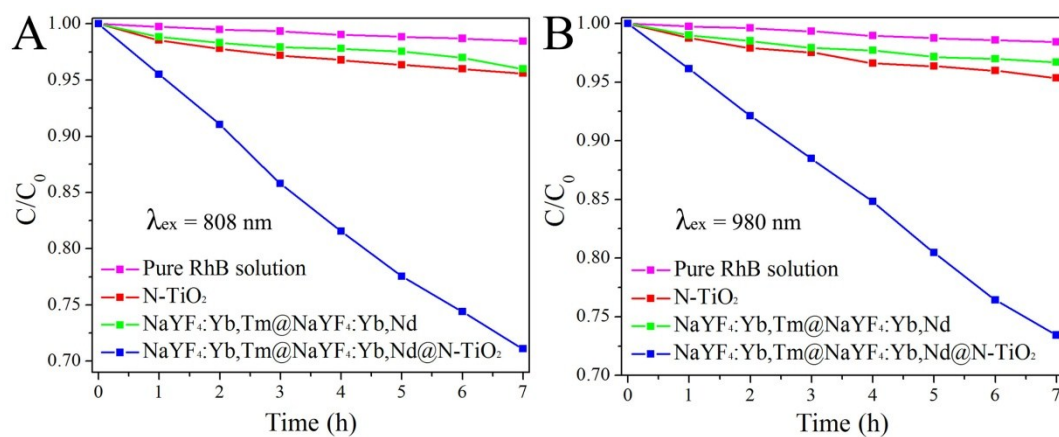


Figure S5. Photocatalytic activities of samples under single NIR diode laser: (A) 808-nm wavelength; (B) 980-nm wavelength. Power density of both lasers is operated at 50 mW/cm².

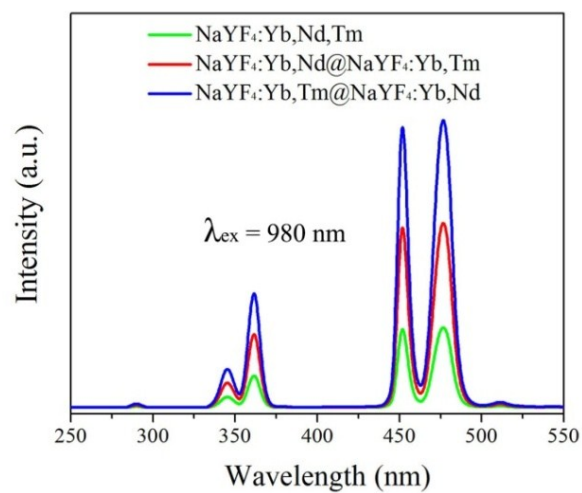


Figure S6. UC spectra of NaYF₄:Yb,Nd,Tm NCs, Nd/Yb@Yb/Tm NCs and Tm/Yb@Yb/Nd NCs under the excitation of 980-nm NIR diode laser.